Original Article

JCBFM

Journal of Cerebral Blood Flow & Metabolism
2021, Vol. 41(10) 2593–2606

DOI: 10.1177/0271678X211007960
journals.sagepub.com/home/jcbfm
SAGE

Neurovascular coupling dysfunction in end-stage renal disease patients related to cognitive impairment

Peng Li[1,2,*], Junya Mu[3,*], Xueying Ma[4], Dun Ding[5], Shaohui Ma[1], Huawen Zhang[2], Jixin Liu[3] and Ming Zhang[1]

Abstract

We aimed to investigate the neurovascular coupling (NVC) dysfunction in end-stage renal disease (ESRD) patients related with cognitive impairment. Twenty-five ESRD patients and 22 healthy controls were enrolled. To assess the NVC dysfunctional pattern, resting-state functional MRI and arterial spin labeling were explored to estimate the coupling of spontaneous neuronal activity and cerebral blood perfusion based on amplitude of low-frequency fluctuation (ALFF)-cerebral blood flow (CBF), fractional ALFF (fALFF)-CBF, regional homogeneity (ReHo)-CBF, and degree centrality (DC)-CBF correlation coefficients. Multivariate partial least-squares correlation and mediation analyses were used to evaluate the relationship among NVC dysfunctional pattern, cognitive impairment and clinical characteristics. The NVC dysfunctional patterns in ESRD patients were significantly decreased in 34 brain regions compared with healthy controls. The decreased fALFF-CBF coefficients in the cingulate gyrus (CG) were associated positively with lower kinetic transfer/volume urea (Kt/V) and lower short-term memory scores, and were negatively associated with higher serum urea. The relationship between Kt/V and memory deficits of ESRD patients was partially mediated by the fALFF-CBF alteration of the CG. These findings reveal the NVC dysfunction may be a potential neural mechanism for cognitive impairment in ESRD. The regional NVC dysfunction may mediate the impact of dialysis adequacy on memory function.

Keywords

End-stage renal disease, cognitive impairment, neurovascular coupling, arterial spin labeling, functional magnetic resonance imaging

Received 30 January 2021; Revised 30 January 2021; Accepted 15 March 2021

Introduction

End-stage renal disease (ESRD) is now recognized as a growing public health problem.[1] It is estimated that 2–3% of the health care budget is allotted to patients with ESRD and could be increased by cognitive impairment.[2] Epidemiological studies found that ESRD patients were vulnerable to vascular damage and local brain region dysfunction,[3] which could lead to cognitive impairment including executive function, memory, and attention.[4,5] However, the neuropathological mechanisms of cognitive impairment in ESRD patients remain largely unknown.

Recently, researchers attributed the cognitive impairment in ESRD patients to the kidney–brain axis disorders.[3,6,7] The kidneys and brain have similar vasoregulatory and anatomic characteristics, with

[1]Department of Medical Imaging, First Affiliated Hospital of Xi'an, Jiaotong University, Xi'an, China
[2]Department of Medical Imaging, Hospital of Shaanxi Nuclear Geology, Xianyang, China
[3]Center for Brain Imaging, School of Life Science and Technology, Xidian University, Xi'an, China
[4]Department of Medical Imaging, The Affiliated Hospital of Inner Mongolia Medical University, Hohhot, China
[5]Department of Medical Imaging, The Second Affiliated Hospital of Xi'an, Jiaotong University, Xi'an, China

*The first two authors contributed equally to this work and should be considered as first co-authors.

Corresponding authors:
Ming Zhang, Department of Medical Imaging, First Affiliated Hospital of Xi'an Jiaotong University, No. 277, West Yanta Road, Xi'an 710061, Shaanxi Province, China.
Email: zhangming01@mail.xjtu.edu.cn

Jixin Liu, Center for Brain Imaging, School of Life Science and Technology, Xidian University, Xi'an, China.
Email: liujixin@xidian.edu.cn

high-volume blood flow and low vascular resistance circulation systems, and they are thus vulnerable to vascular damage.[7] Many of the known traditional risk factors (including hypertension, aging, and diabetes mellitus), nontraditional risk factors (including chronic inflammation, oxidative stress, and hypercoagulable state), and uremic toxins (including hyperhomocysteinemia, guanidine compounds, and cystatin-C) mainly result in cerebral vascular injury, endothelial dysfunction, direct neuronal toxicity, and eventually lead to cognitive impairment in ESRD patients.[3] In addition, maintenance dialysis can also contribute to cerebral hyperperfusion and hypoperfusion, cerebral edema, cerebral ischemia and cerebrovascular disease by inducing hemodynamic instability, fluctuating uremic toxin titers, fluid shifts, and direct neurotoxicity.[8,9]

To sustain normal neuronal function, the brain has developed a tight temporal and regional coupling called "neurovascular coupling (NVC)" mechanism, that refers to brain regions with stronger connectivity that tend to have higher intrinsic neuronal activities with more energy consumption, that resulted in increased cerebral blood flow (CBF).[10] The NVC dysfunction is suggested to play an important role in the neuropathological mechanism for both neurological and psychiatric disorders.[11–15] Multimodal neuroimaging has been established as a valuable tool for the identification of the neuropathologic mechanisms of cognitive impairment in patients with ESRD.[16–23] ESRD patients undergoing hemodialysis (HD) and peritoneal dialysis exhibited elevated CBF over the brain region compared with healthy controls,[16,17] but decreased regional CBF mainly in the anterior cingulate cortex compared with nondialysis ESRD patients.[17] By analyzing multiple aspects of blood oxygen level dependent (BOLD) signals,[24] including the amplitudes of low-frequency fluctuation (ALFF), fractional ALFF (fALFF), regional homogeneity (ReHo), and degree centrality (DC), resting-state functional MRI (rs-fMRI) has become a useful and objective tool for identifying neuronal activity abnormalities characteristic of cognitive impairments in ESRD patients.[18–23] For example, changed ALFF and ReHo values mainly in default mode network (DMN) region have been found to reveal abnormal spontaneous neuronal activity in ESRD patients.[19,20] However, previous studies mainly focused on neural activity or cerebral perfusion, that could not reflect comprehensively the NVC dysfunction expressed in the form of an incoordination between neural activity and CBF in ESRD patients. Moreover, the spatial inconsistency between changed cerebral perfusion and abnormal spontaneous neuronal activity makes it difficult for nephrologists and neuropsychiatrists to elucidate the neuropathologic mechanisms of NVC dysfunctional patterns underlying cognitive impairment in patients with ESRD.

In the present study, we conducted a series of multimodal neuroimaging analyses to verify three hypotheses. Firstly, the NVC dysfunction was manifested in ESRD patients. Secondly, the NVC dysfunction was associated with cognitive impairment. Finally, the NVC dysfunction mediated links between the clinical characteristics of ESRD and cognitive impairment. To address these hypotheses, four types of NVC patterns[15] (including ALFF-CBF, fALFF-CBF, ReHo-CBF, and DC-CBF correlation coefficients) reflected the NVC dysfunction in ESRD patients. The BOLD signals (ALFF, fALFF, ReHo, and DC) represented the oxygen uptake ability of neurons from different aspects of neuroimaging. Consequently, the NVC patterns[15] (ALFF-CBF, fALFF-CBF, ReHo-CBF and DC-CBF correlation coefficients) reflect the coordination between the requirement of oxygen and the blood supply, that is the function of NVC.[25] Partial least-squares correlation analysis (PLSC) and mediation analysis were used to evaluate the relationship among the NVC pattern's alteration, cognitive impairment, and the clinical characteristics in ESRD patients.

Materials and methods

Participants

This study was approved by the Research Ethics Review Board of the First Ailiated Hospital of Xi'an Jiaotong University (Approval No. 2020G64) and was conducted in accordance with the Declaration of Helsinki. All participants provided written informed consent. From April 2019 to April 2020, 31 right-handed ESRD patients who underwent maintenance HD were recruited. Data from four male and two female patients were excluded owing to head-movement induced artifacts during the MRI scans. Hence, imaging data of 25 patients were included for statistical analysis (18 males and seven females). The dialysis durations for all ESRD patients were longer than three months. The exclusion criteria included: (1) ages less than 18 years, (2) psychiatric or neurodegenerative disorders, (3) history of type I or II diabetes mellitus, (4) history of alcohol or drug abuse, (5) any evidence of brain lesions (hemorrhage, stroke, tumor, encephalomalacia, and head trauma) identified from the medical history or during conventional MRI scans, (6) clinically relevant visual and auditory disturbances, such as blurred vision, hearing loss, and other clinically relevant symptoms that cannot be assessed with neuropsychological scales, or (7) claustrophobia.

Twenty-two demographically similar healthy controls (HCs) (14 males and 8 females) who had no

relevant medical history or neurological diseases were recruited from the local community with advertisements.

Clinical characteristics

Demographic, medication details and clinical data were collected from the medical records of ESRD patients. Furthermore, blood biochemical tests were conducted in all patients with ESRD on the day before HD treatment. To ensure the adequacy of dialysis, the average dialysis time in the consecutive three months in all ESRD patients was approximately 4 h. The kinetic transfer/volume urea measurements (Kt/V) were calculated by averaging values from consecutive three-month recordings prior to MR imaging in all ESRD patients. Twenty patients were dialyzed three times per week, and five patients were dialyzed five times every two weeks. The main underlying cause of ESRD in our patients' group was glomerulonephritis (21 patients), two patients were immunoglobulin A (IgA) nephropathy, and two patients were membranous nephropathy. The HCs participants did not undergo blood biochemical tests (Table 1).

Neuropsychological assessment

Neuropsychological assessments were performed in all subjects before the MR scan on the day before HD treatment. The Montreal cognitive assessment (MoCA) test[26] was applied as a screening instrument for global cognitive function, including the domains of visuospatial skills, attention, memory, orientation, language, executive function, conceptual thinking, and calculation. The auditory verbal learning test–Huashan version (AVLT-H) was performed to evaluate participant's verbal working memory (immediate recall total score, IR-S), short-term delayed memory (short-term delayed recall score, SR-S), long-term delayed memory (long-term delayed recall score, LR-S), and recognition (recognition score, REC-S). AVLT-H has demonstrated to be acceptable to Mandarin speakers and is sensitive to the detection of memory deficits in mild cognitive impairments.[27] The trail-making test (TMT)[28]were performed to evaluate participant's visual–spatial orientation, attention, psychomotor speed, and executive function (Table 2).

Moreover, the Beck anxiety inventory (BAI) and the Beck depreesion inventory (BDI) were performed to evaluate participant's mood disorder.[29] The Pittsburgh's sleep quality index (PSQI) scale was used to evaluate participant's sleep dysfunction[30] (Table 2).

MRI data acquisition

Within 1 h after the neuropsychological assessment, MRI data was obtained with a 3.0 T GE discovery MR750 scanner with an eight channel phased array head coil. Foam padding was used to minimize head motion, and ear plugs were used to reduce scanner noise. All participants were instructed to keep their eyes closed, and to relax without falling asleep during the acquisition period. After the MRI scan, all participants were asked questions to verify their cooperation.

Conventional protocols

Individual high-resolution T1-weighted structural images were collected with a three-dimensional brain volume imaging sequence (3D-BRAVO) with the following scan parameters: echo time (TE) = 3.2 ms, repetition time (TR) = 8.2 ms, flip angle (FA) = 15°, matrix = 256 × 256, slice thickness = 1 mm, and slices number = 140. Clinical T1-fluid attenuated inversion recovery images (T1-FLAIR: TE/TR = 24/1750 ms, TI = 780 ms, FA = 111°, matrix = 256 × 256, slice thickness = 6 mm, and slice gap = 0.6 mm), T2-weighted periodically rotated overlapping parallel lines with enhanced reconstruction (PROPELLER) images (TE/TR = 84/9638 ms, refocus angle = 142°, matrix = 256 × 256, slice thickness = 6 mm, and gap = 0.6 mm) were obtained to exclude intracranial lesions. The conventional protocols were scanned before 3D pseudocontinuous arterial spin labeling (3D-pCASL) and rs-fMRI to allow the participant to adapt to the MRI environment, and then assessed the participant's needs once again. We ended the scans in the instance(s) any participant(s) did not cooperate with the completion of the MRI scan.

rs-fMRI

The rs-fMRI data were collected with an echo-planar imaging sequence which was sensitive to BOLD contrast (TE = 50 ms, TR = 2000 ms, FA = 90°, field-of-view (FOV) = 240 × 240 mm^2, matrix = 64 × 64, voxel size = 3 × 3 × 3 mm^3, slices = 45, slices thickness = 4 mm, slice gap = 0 mm). Each scan lasted 6 min 10 s and included 185 functional volumes. After the rs-fMRI scan, all participants were asked to ensure if they were awake during the scan.

3D-Pcasl images

ASL is a noninvasive MRI perfusion technique used to evaluate cerebral hyperperfusion and hypoperfusion in ESRD patients without introducing exogenous contrast agents or radiation exposure.[16,17] According to the consensus statement of the International Society

Table 1. Demographic information and clinical characteristics in ESRD patients and healthy control subjects (HCs).

Variable	HCs ($n = 22$)	ESRD patients ($n = 25$)		*t*-value	*p*-value
Age (years)	31.18 (10.54) (26.51, 35.86)	33.68 (8.38) (30.22, 37.14)		–0.905	0.37[a]
Gender (M/F)	14 (8)	18 (7)		0.377	0.539[b]
Education (years)	12.41 (2.77) (11.18, 13.63)	11.28 (2.94) (10.07, 12.49)		1.355	0.182[a]
Dialysis vintage (months)	/	32.45 (26.45) (23.56, 45.40)		/	/
Creatinine (μmol/L)	/	939.76 (254.83) (834.57, 1044.95)		/	/
Urea (mmol/L)	/	23.48 (8.48) (19.98, 26.98)		/	/
Kt/V	/	1.46 (0.21) (1.38, 1.55)		/	/
Hemoglobin (g/L)	/	102.44 (20.57) (93.95, 110.93)		/	/
Hematocrit (%)	/	32.65 (6.39) (30.02, 35.29)		/	/
Cystatin C (μg/mL)	/	4.59 (1.31) (4.05, 5.13)		/	/
Potassium (mmol/L)	/	4.98 (0.73) (4.68, 5.28)		/	/
Sodium (mmol/L)	/	144.48 (3.15) (143.18, 145.78)		/	/
Phosphorus (mmol/L)	/	1.78 (0.40) (1.62, 1.95)		/	/
Calcium (mmol/L)	/	2.12 (0.21) (2.04, 2.22)		/	/
Parathormone (ng/L)	/	747.72 (468.41) (554.37, 941.07)		/	/
Medication		*N*	%		
AT1-blocker		14	56	/	/
Beta-blocker		13	52	/	/
EPO		23	92	/	/
Antidepressants		0	0	/	/
Antihistamines		0	0	/	/
Analgesics		0	0	/	/
Vitamin D		17	68	/	/
Calcium antagonists		9	36	/	/

ESRD: end-stage renal disease.

Note: Unless otherwise indicated, data were reported as mean (standard deviation) (95% confidence interval).

[a]Analyzed with the independent two-sample *t* test; data in parentheses have a 95% confidence interval.

[b]Analyzed with the chi-square test.

for Magnetic Resonance in Medicine perfusion study group,[31,32] perfusion images were obtained using a 3 D-pCASL technique (TR = 5046 ms, TE = 11 ms, slices = 50, postlabel delay = 2025 ms, FA = 111°, slice thickness = 3 mm, FOV = 256 × 256 mm,^{2} matrix = 128 × 128). Each scan lasted 4 min.

Functional imaging analysis

3D-Pcasl analysis. Data were preprocessed using the Functional Magnetic Resonance Imaging of the Brain Software Library (FSL v6.0.3, http://www.fmrib.ox.ac.uk/fsl) and Statistical Parametric Mapping (SPM8, http://www. fil.ion.ucl.ac.uk/spm). First, the 3D-pCASL and 3D-BRAVO data were corrected for gradient nonlinearities in all directions, realignment, segmentation and coregistration. Second, ASL images were registered to the brain extracted from the 3D-BRAVO data. Mean whole-brain CBF values were calculated and converted to quantitative CBF maps with the unit of mL/100 g/min in the mask. Third, outcomes were normalized to the Montreal's Neurological Institute (MNI) space. Subsequently,

Table 2. Neuropsychological assessment in ESRD patients and Healthy control subjects (HCs).

Variable	HCs ($n = 22$)	ESRD patients ($n = 25$)	Unadjusted *t*-value	Unadjusted *p*-value	Adjusted *t*-value	Adjusted *p*-value
AVLT-H						
IR-S	26.91 (4.02) (25.12, 28.69)	23.64 (4.41) (21.82, 25.46)	2.71	0.008[a,b]	2.64	0.01[a,b]
SR-S	10.50 (1.34) (9.91, 11.09)	9.04 (1.79) (8.30, 9.78)	2.69	0.009[a,b]	3.13	0.003[a,b]
LR-S	10.41 (1.33) (9.82, 11.00)	8.00(1.66) (7.32, 8.68)	5.32	<0.001[a,b]	5.43	<0.001[a,b]
REC-S	11.77 (0.53) (11.53, 12.00)	11.2 (0.96) (10.80, 11.60)	3.13	0.003[a,b]	2.49	0.017[a,b]
MoCA	26.64 (2.85) (25.37, 27.90)	24.08 (2.55) (23.03, 25.13)	5.08	<0.001[a,b]	3.24	0.002[a,b]
TMT	44.68 (13.72) (38.60, 50.77)	59.80 (30.6) (47.17, 72.43)	–2.64	0.007[a,b]	–2.13	0.038[a,b]
BAI	24.77 (2.56) (23.64, 25.91)	30.52 (6.43) (27.87, 33.17)	–4.26	<0.001[a,b]	–3.92	<0.001[a,b]
BDI	7.77 (5.57) (5.30, 10.24)	18.20 (12.35) (13.10, 23.30)	–4.48	<0.001[a,b]	–3.64	0.001[a,b]
PSQI	3.27 (1.61) (2.56, 3.99)	5.72 (3.47) (4.29, 7.15)	–3.68	0.001[a,b]	–3.03	0.004[a,b]

AVLT-H: auditory verbal learning test–Huashan version; IR-S: immediate recall total score; SR-S: short-term delayed recall score; LR-S: long-term delayed recall score; REC-S: recognition score; MoCA: Montreal cognitive assessment; TMT: trail-making test; BAI: Beck anxiety inventory; BDI: Beck depreesion inventory; PSQI: Pittsburgh's sleep quality index.
Data were reported as mean (standard deviation) (95% confidence interval).
[a]Analyzed with the two-sample *t* test; data in parentheses have a 95% confidence interval after controlling age, sex and education level.
[b]Indicates a statistically significant difference.

smoothing was performed with an isotropic Gaussian kernel of 8 mm (full-width-at-half-maximum, FWHM).

BOLD signals preprocessing

Data were preprocessed using SPM8 (http://www. fil. ion.ucl.ac.uk/spm) and Data Processing Assistant for Resting-State fMRI toolbox[33] (DPARSF, http://www. restfmri.net/forum/DPARSF). First, the first 10 volumes of functional images were discarded. Second, the remaining images were corrected for temporal shifts between head movement (24 motion-related regression) and slices (a least-squares approach).[34] Third, the realigned images were spatially normalized to the MNI template. The resultant normalized functional images were then transformed to the Z value and smoothed with a Gaussian kernel (FWHM = 8 mm). Finally, a bandpass filtering of only the frequency within range of 0.01 and 0.1 Hz was applied to keep low-frequency fluctuations.

ALFF, fALFF, ReHo, and DC analyses

The ALFF, fALFF, ReHo, and DC maps were calculated using DPARSF.[33] For ALFF and fALFF, the time course for each given voxel was decomposed into the frequency domain with the fast Fourier transform (FFT). The ALFF value was calculated as the average square root of the power spectrum following the application of the FFT across the frequency range of 0.01–0.08 Hz for each voxel. The fALFF value was calculated as the ratio of the power in the specific frequency band (bandpass filtering in the range of 0.01–0.08 Hz) to reduce the influence of frequency ranges of nonspecific signals. To eliminate the differences of whole-brain fALFF in the overall level between individuals, the fALFF value of each voxel was normalized to the Z value.

For the ReHo map, bandpass filtering (0.01–0.08 Hz) on the normalized images was performed. ReHo values were quantified by calculating the Kendall's coefficient of concordance value between a given voxel and its neighbors in a voxel-wise way.[35] The ReHo value of each voxel was divided by the global average value of the ReHo map to reduce the influence of individual variability. Finally, spatial smoothing was conducted with an 8 mm FWHM Gaussian kernel.

For the DC map, a voxel-based whole-brain correlation analysis was computed on the preprocessed rs-fMRI data. In the grey matter (GM) mask, the time course of each voxel was correlated to each voxel time course. Thus, an $n \times n$ matrix of Pearson's correlation

coefficients between any pair of voxels was acquired, where n is the voxel number of the GM mask. By thresholding each correlation at $r > 0.25$,[36] we transformed the Pearson's correlation data into normally distributed Fisher Z-scores and constructed the whole-brain functional network. In the present study, only positive Pearson's correlation coefficients were considered. For a given voxel, the DC was computed as the sum of the significant connections at the individual level. The DC map indicates the number of functional connections for a given voxel in the voxel-based graphs at the individual level, which has been extensively used to represent the node characteristics of large-scale brain intrinsic connectivity networks.[37]

Whole GM-based NVC analysis

To quantitatively evaluate the NVC, whole GM correlation was performed between images of neuronal activity (averaged ALFF, fALFF, ReHo, DC maps) and cerebral perfusion (averaged CBF maps). For each individual, four neurovascular patterns were assessed (ALFF-CBF, fALFF-CBF, ReHo-CBF and DC-CBF coefficients) at the whole GM level (Supplementary Fig. 1).

Brain region-based NVC analysis

The Human Brainnetome Atlas (http://atlas.brainnetome.org) was used to segregate the cerebrum into 246 independent regions. This provided a fine-grained, cross-validated atlas that contained information on both anatomical and functional connections.[38] The correlation coefficient between the neuronal activity and cerebral perfusion was calculated for each brain region, and four brain region-based neurovascular patterns were assessed (ALFF-CBF, fALFF-CBF, ReHo-CBF and DC-CBF coefficients) (Supplementary Fig. 1).

Statistical analysis

Between-group difference of clinical characteristics and cognitive variables. The between-group differences in the subjects' demographics (age, educational level), clinical blood biochemistry tests (Kt/V, creatinine, urea, hemoglobin, hematocrit, cystatin C, potassium, sodium, phosphorus, calcium, and parathormone), and cognitive variables (MoCA, IR-S, SR-S, LR-S, REC-S, TMT, BAI, BDI, and PSQI) were compared with the Kolmogorov–Smirnov, Levene's and independent two-sample t-tests (Levene's test for determining the equality of variances, Kolmogorov–Smirnov test for normality, and Student's t-test for equality of means) using SPSS (version 20.0, SPSS Statistics, IBM, Armonk, NY). The difference of gender-ratio was analyzed with the Chi-square test. A multiple linear regression analysis was used to eliminate the impact of age, educational level, and sex between-group differences of cognitive test results. All p values less than 0.05 were regarded as statistically significant.

Between-group comparison of ALFF, fALFF, ReHo, DC, and CBF. A two-sample t test were implemented to test the group differences of ALFF, fALFF, ReHo, DC, and CBF maps at the whole brain GM level and the Human Brainnetome Atlas, respectively. A false discovery rate (FDR) correction was applied for multiple comparison corrections at Human Brainnetome Atlas level; $p < 0.05$ was considered statistically significant. A Bonferroni correction was applied for multiple comparison corrections at whole brain GM level ($p = 0.05/5$, corresponding to $p = 0.01$).

Between-group differences of NVC pattern. Four types of NVC patterns (ALFF-CBF, fALFF-CBF, ReHo-CBF, and DC-CBF coefficients) were compared between ESRD and HCs groups at the whole brain GM level and the Human Brainnetome Atlas level, respectively. At the whole GM level, whole GM correlation was performed between neuronal activity images and cerebral perfusion images. For each individual, four types of whole GM-based NVC pattern were assessed (ALFF-CBF, fALFF-CBF, ReHo-CBF, and DC-CBF coefficients). Then these NVC coefficients were compared between ESRD group and HCs by using a two-sample t-test. A Bonferroni correction was applied to account for testing four types of NVC patterns at the whole brain GM level ($p = 0.05/4$, corresponding to $p = 0.0125$).

At the Human Brainnetome Atlas level (246 brain regions), the correlation coefficient between neuronal activity and cerebral perfusion was calculated for each brain region. Then these correlation coefficients were compared between ESRD group and HCs by using a two-sample t-test. An FDR correction was applied for multiple comparison corrections at brain regions level; $p < 0.05$ was considered statistically significant. To correct for multiple comparisons in measurements, a Bonferroni correction was applied to account for testing four types of NVC patterns ($p = 0.05/4$, corresponding to $p = 0.0125$). Therefore, the significance threshold was set at $p < 0.01$.

Multivariate PLSC analysis between the NVC pattern's alteration, the cognitive variables and clinical characteristics. Multivariate PLSC analysis (graphical user interface, Rotman Research Institute, Baycrest Centre, University of Toronto; downloaded from http://www.rotman-baycrest.on.ca/pls/ running on MATLAB (R2013b, MathWorks, Inc., Natick, MA, USA)) was

used to explore co-variations between the NVC pattern's alteration (ALFF-CBF, fALFF-CBF, ReHo-CBF, and DC-CBF coefficients), the cognitive variables (MoCA, IR-S, SR-S, LR-S, REC-S, and TMT), and clinical blood biochemistry tests (Kt/V, creatinine, urea, hemoglobin, hematocrit, cystatin C, potassium, sodium, phosphorus, calcium, and parathormone) in ESRD patients. We can obtain six pairs of latent variables (LVs) with corresponding singular values [representing the proportion of the covariance accounted for by the given LV (the cross-block covariance)] and saliences (indicating the degree to which each variable was related to the effect characterized by that LV).

However, the results might be confused by several factors, which include age,[39] gender,[40] and education level.[41] Furthermore, the mood disorder and sleep quality of ESRD patients also have influences on cognitive assessments.[21] Therefore, we corrected our data manually with multiple linear regressions to eliminate the impact before we conducted our main analyses.

Mediation analysis. To examine the effects of clinical blood biochemistry indicators on cognitive variables and NVC pattern's alteration in ESRD patients, we performed mediation analyses to identify if the NVC pattern's alteration could mediate the role of clinical indicators in cognitive impairment.

Based on the results of the PLSC analysis, clinical blood biochemistry indicators constituted the independent variable, cognitive impairment measurements indicated the dependent variable and the NVC pattern's alteration consisted of the mediator variable. The mediation analyses were performed with SPSS 20.0. The significance threshold for the Sobel test was set at $p < 0.05$.

Results

Demographic, clinical blood biochemistry tests and neuropsychological results

The demographic, medication details and clinical data for each group are listed in Table 1. No significant differences in age, gender, or educational levels were observed between groups. In terms of neuropsychological tests (Table 2), poorer performance was found in ESRD patients in three subitems of AVLT-H, i.e., IR-S ($p = 0.010$), SR-S ($p = 0.003$), LR-S ($p < 0.001$), and REC-S ($p = 0.017$) compared with the HCs group. Furthermore, poorer performance was found in ESRD patients in MoCA ($p = 0.002$), TMT ($p = 0.038$), BAI ($p < 0.001$), BDI ($p = 0.001$), and PSQI ($p = 0.004$) compared with the HCs group.

Between-group comparison of ALFF, fALFF, ReHo, DC, and CBF

The spatial distribution of averaged CBF, ALFF, fALFF, ReHo, and DC maps in HCs and ESRD group are shown in Supplementary Fig. 2, the HCs and ESRD patients had similar spatial distribution. At the whole brain GM level, the ESRD patients showed increased averaged CBF and decreased BLOD signals (averaged ALFF, fALFF, ReHo, and DC) compared with HCs. At the Human Brainnetome Atlas level, the ESRD patients showed increased CBF values and decreased BLOD signals (ALFF, fALFF, ReHo, and DC) in multiple brain regions compared with HCs. The between-group comparison of ALFF, fALFF, ReHo, DC, and CBF maps at both the whole brain GM level and the Human Brainnetome Atlas level are shown in supplementary materials (Supplementary Fig. 3).

Between-group whole GM-based NVC comparison

No significant differences were found between groups regarding the ALFF-CBF, fALFF-CBF, ReHo-CBF and DC-CBF coefficient maps at the whole brain GM level.

Between-group brain region-based NVC comparison

In the ALFF-CBF maps, significant between-group differences were found in 22 brain regions of the Human Brainnetome Atlas, as shown in Figure 1(a) and Supplementary Table S1. These included the left superior frontal gyrus (SFG), left middle frontal gyrus (MFG), left orbital gyrus (OrG), left precentral gyrus (PrG), left superior temporal gyrus (STG), left middle temporal gyrus (MTG), bilateral fusiform gyrus (FuG), bilateral insular gyrus (INS), bilateral cingulate gyrus (CG), right medioventral occipital cortex (MVOcC), left lateral occipital cortex (LOcC), left amygdala (Amyg), left basal ganglia (BG), and right thalamus (Tha) ($p < 0.01$ after FDR correction).

In the fALFF-CBF maps, significant differences were found between-group in 14 brain regions of the Human Brainnetome Atlas, as showed in Figure 1(b) and Supplementary Table S2. These included the left SFG, right MFG, left OrG, left STG, bilateral MTG, right inferior temporal gyrus (ITG), right FuG, left inferior parietal lobule (IPL), bilateral CG, and left BG ($p < 0.01$ after FDR correction).

In the ReHo-CBF maps, significant differences were found between-group in eight brain regions of the Human Brainnetome Atlas, as shown in Figure 1(c) and Supplementary Table S3. These included the left

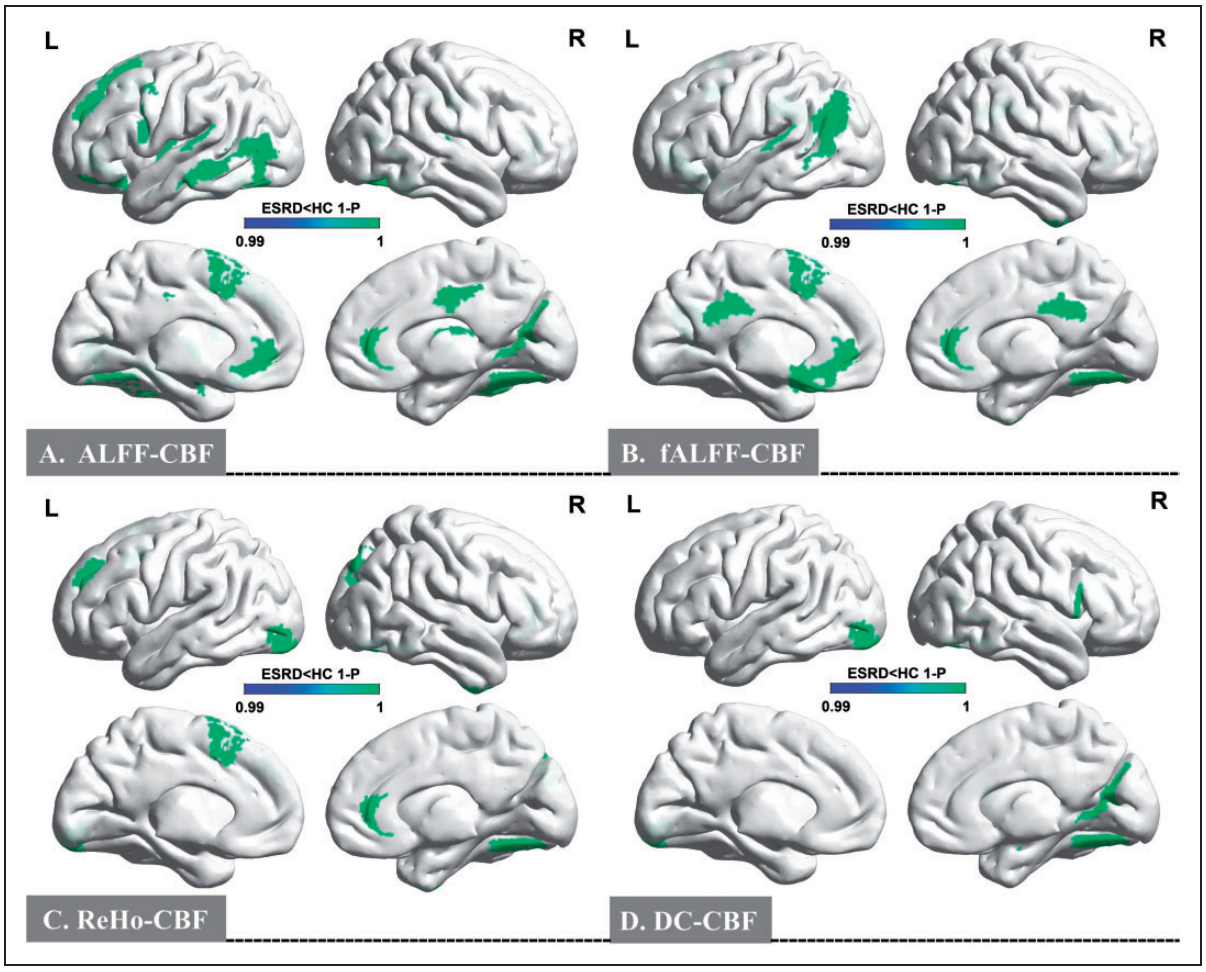

Figure 1. Spatial distribution maps between-group differences of the four types of NVC patterns. In comparison with HCs, ESRD patients showed significantly lower ALFF-CBF, fALFF-CBF, ReHo-CBF, and DC-CBF coefficients in 34 brain regions at the Human Brainnetome Atlas ($p < 0.01$, FDR correction).
NVC: neurovascular coupling; ALFF: amplitude of low-frequency fluctuation; fALFF: fractional ALFF; ReHo: regional homogeneity; DC: degree centrality; HCs: healthy control subjects; ESRD: end-stage renal disease; FDR: false discovery rate.

SFG, left MFG, right inferior frontal gyrus (IFG), right FuG, right CG, bilateral LOcC, and left Tha ($p < 0.01$ after FDR correction).

In the DC-CBF maps, significant differences were found between-group in five brain regions of the Human Brainnetome Atlas, as shown in Figure 1(d) and Supplementary Table S4. These included the right IFG, right FuG, right MVOcC, left LOcC, and right Amyg ($p < 0.01$ after FDR correction).

The NVC patterns in ESRD patients were significantly decreased in 34 brain regions at the Human Brainnetome Atlas compared with the HCs group. The averaged correlation coefficients and corresponding standard deviations of four types of brain region-based NVC patterns in all participants were calculated and are shown in Supplementary Fig. 4.

Multivariate PLSC analysis

Multivariate PLSC between the NVC pattern's alteration and clinical blood biochemistry tests. Multivariate PLSC analysis correlating the NVC pattern's alteration to clinical blood biochemistry tests revealed one significant LV ($p < 0.05$) which accounted for 38.16% of the cross-block covariance. The pattern identified by the LV showed that lower fALFF-CBF coefficients in the CG were associated positively with lower Kt/V, and were negatively associated with higher serum urea in ESRD patients (Figure 2).

Multivariate PLSC analysis between the NVC pattern's alteration and cognitive variables. Multivariate PLSC analysis correlating the NVC pattern's alteration to cognitive variables revealed one significant LV ($p < 0.05$) which accounted for 46.70% of the cross-block

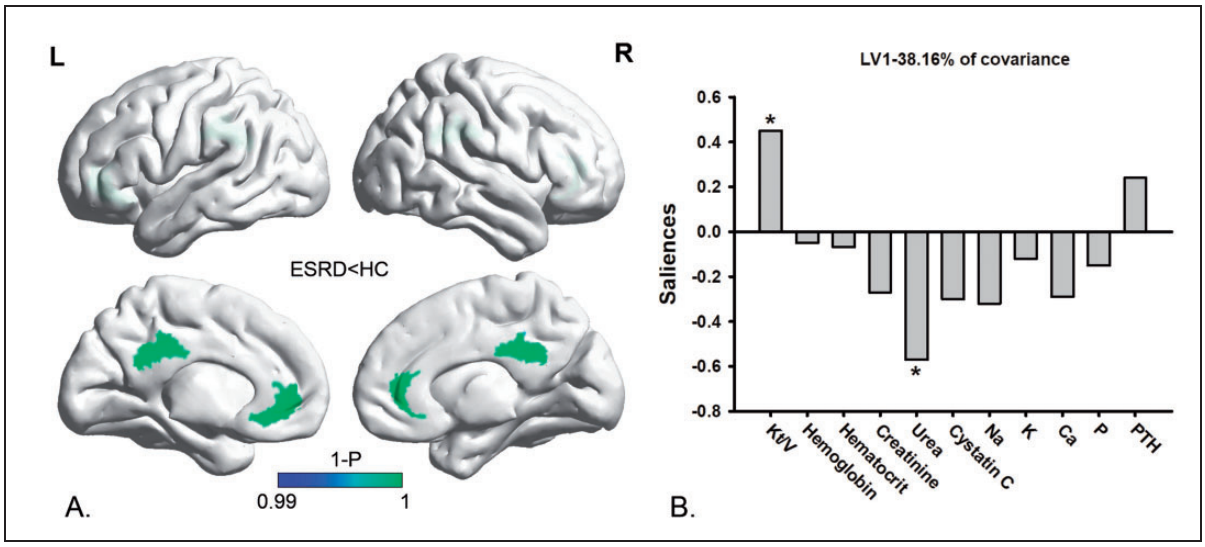

Figure 2. Multivariate PLSC analysis between the NVC pattern alteration and clinical blood biochemistry tests in ESRD patients. Multivariate PLSC analysis correlating the NVC pattern alteration to clinical blood biochemistry tests revealed one significant LV ($p < 0.05$) which accounted for 38.16% of the cross-block covariance. The pattern identified by the LV showed that the lower fALFF-CBF coefficients in the CG (section (a)) were positively associated with lower Kt/V values, and were negatively associated with higher serum urea (section (b)).
PLSC: partial least-squares correlation; NVC: neurovascular coupling; fALFF: fractional amplitude of low-frequency fluctuation; CBF: cerebral blood flow; LV: latent variable; CG: cingulate gyrus; Kt/V: kinetic transfer/volume urea; ESRD: end-stage renal disease.

covariance. The pattern identified by the LV showed that lower fALFF-CBF coefficients in the CG were associated positively with lower short-term memory functional scores (lower SR-S) in ESRD patients (Figure 3).

Multivariate PLSC between the clinical blood biochemistry tests and cognitive variables. Multivariate PLSC analysis correlating the clinical blood biochemistry tests to cognitive variables revealed one significant LV ($p < 0.05$) which accounted for 73.50% of the cross-block covariance. The pattern identified by the LV showed that lower Kt/V and hemoglobin were associated positively with lower short-term memory function scores (lower IR-S and SR-S) in ESRD patients (Figure 4).

Mediation analysis. To examine the relationship among NVC pattern's alteration, clinical blood biochemistry indicators and cognitive variables in ESRD patients, we performed mediation analysis to identify if the NVC pattern's alteration could mediate the role of clinical indicators in cognitive impairment. Based on the results of the PLSC analysis, the independent factor was Kt/V and the dependent variable was short-term memory function indicator that were reflected by the SR-S, with the fALFF-CBF coefficient in the CG as the proposed mediator based on the results of PLSC. As shown in Figure 5, the mediation analysis indicated that lower fALFF-CBF coefficients in the CG partially mediated the effects of Kt/V on the short-term memory function deficits ($c' = 0.698$, $p = 0.003$) in ESRD patients.

Discussion

Main findings

We aimed to investigate the NVC dysfunction in ESRD patients related with cognitive impairment by exploring the multimodal neuroimaging relationship between the instrinct neuronal activity and the corresponding cerebral blood perfusion. Consistent with our hypothesis, the NVC patterns in ESRD patients were significantly decreased in 34 brain regions at the Human Brainnetome Atlas compared with the HCs. The decreased fALFF-CBF outcomes in CG were positively associated with lower Kt/V and lower short-term memory function, negatively associated with higher serum urea in ESRD patients. Mediation analysis proved that the relationship between Kt/V and memory deficits of ESRD patients was partially mediated by the fALFF-CBF alteration of the CG.

Potential physiological meanings of NVC dysfunction

Previous neuroimaging studies[16–23] have discovered the reduced neural activity, changed cerebral perfusion in multiple regions, and related cognitive impairment in ESRD patients, based on the analyses of multiple

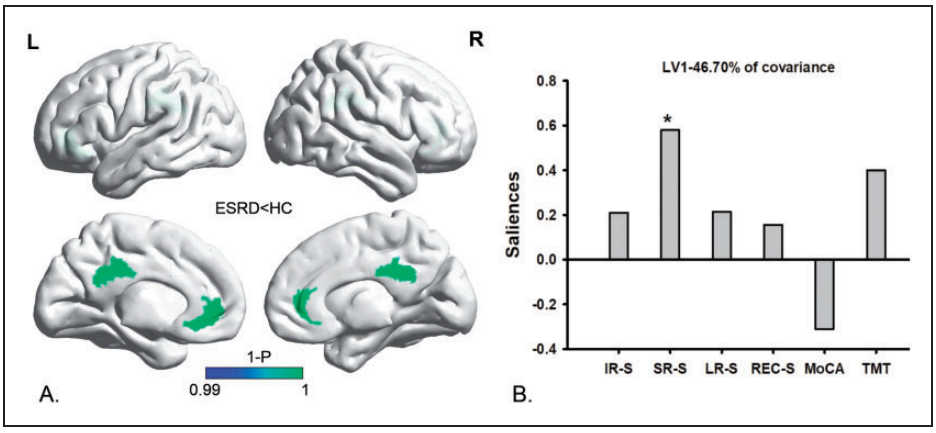

Figure 3. Multivariate PLSC analysis between the NVC pattern's alteration and cognitive variables in ESRD patients. Multivariate PLSC analysis correlating the NVC pattern's alteration to cognitive variables revealed one significant LV ($p < 0.05$), which accounted for 46.70% of the cross-block covariance. The pattern identified by the LV showed that lower fALFF-CBF coefficients in the CG (section (a)) were positively associated with lower SR-S values (section (b)).
PLSC: partial least-squares correlation; NVC: neurovascular coupling; fALFF: fractional amplitude of low-frequency fluctuation; CBF: cerebral blood flow; CG: cingulate gyrus; LV: latent variable; SR-S: short-term delayed recall score; ESRD: end-stage renal disease.

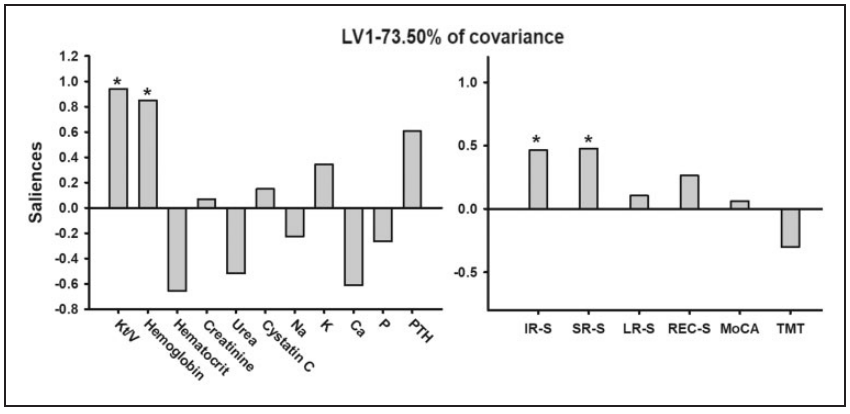

Figure 4. Multivariate PLSC analysis between the clinical blood biochemistry tests and cognitive variables. Multivariate PLSC analysis correlating the clinical blood biochemistry tests to cognitive variables revealed one significant LV ($p < 0.05$), which accounted for 73.50% of the cross-block covariance. The pattern identified by the LV showed that lower Kt/V and hemoglobin were positively associated with lower IR-S and SR-S values in ESRD patients.
PLSC: partial least-squares correlation; LV: latent variable; Kt/V: kinetic transfer/volume urea; IR-S: immediate recall total score; SR-S: short-term delayed recall score; ESRD: end-stage renal disease.

aspects of BOLD signals (ALFF, fALFF, ReHo, and DC) and the ASL technique (CBF). ALFF[42] is defined as the total power within the low-frequency range (between 0.01–0.1 Hz), while fALFF[43] is defined as the relative contribution of specific low-frequency (0.01–0.1 Hz) fluctuation to the entire detectable frequency range. ReHo[35] measures the functional coherence of a given voxel with its nearest neighbors based on the hypothesis that significant neural activities would more likely occur in clusters rather than in a single voxel. DC[44] is the summation of correlation coefficients in the brain between one voxel and all other voxels, which reflect the corresponding blood supply and metabolism of brain hubs. Therefore, the NVC patterns (ALFF-CBF, fALFF-CBF, ReHo-CBF, and DC-CBF coefficients) reflect the coordination between blood supply and oxygen demand in various aspects of the BOLD signal.[15] The NVC ensures that the brain has a proportionally matched CBF response to neural activity, whereas the dysfunction of the NVC—irrespective of whether it was caused by aging itself or pathology—can lead to additional cerebral pathologies and neurological disorders.[45]

Our results indicated that the NVC patterns in ESRD patients were significantly decreased in 34

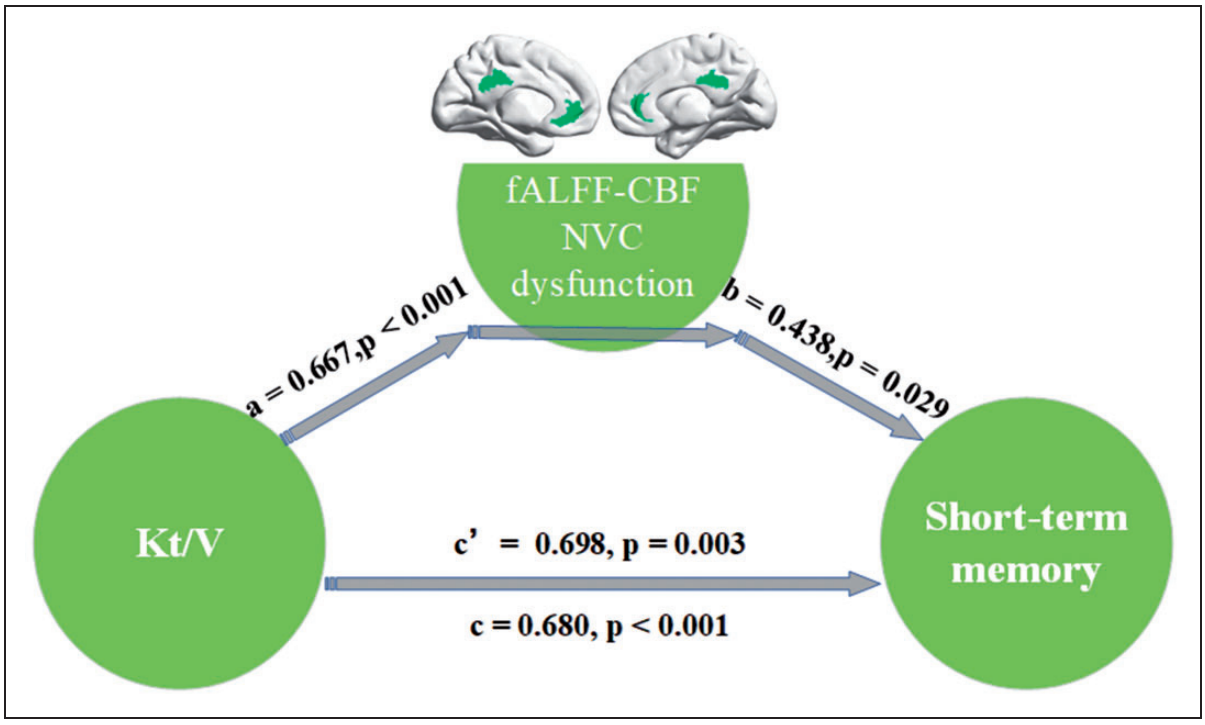

Figure 5. Mediation analysis. In the mediation analysis, the independent factor was Kt/V and the dependent variable was a short-term memory function indicator. These were reflected by the SR-S, while the fALFF-CBF coefficient in the CG served as the proposed mediator. The mediation analysis result indicated that NVC dysfunction (lower fALFF-CBF coefficient) in the CG partially mediated the effect of Kt/V on the short-term memory function deficits ($c' = 0.698$, $p = 0.003$) in ESRD patients.
Kt/V: kinetic transfer/volume urea; NVC: neurovascular coupling; fALFF: fractional amplitude of low-frequency fluctuation; CBF: cerebral blood flow; CG: cingulate gyrus; SR-S: short-term delayed recall score; ESRD: end-stage renal disease.

brain regions compared with HCs. These brain regions with the NVC dysfunction included frontal, temporal, parietal, occipital, and basal ganglia regions, and indicated widespread mismatch between the requirement of oxygen and the blood supply in ESRD patients, that is, widespread dysfunction of neurovascular units. In Alzheimer's disease patients,[46] to meet sufficiently adequate metabolic demands, impaired blood flow responses to neural activity as a result of the NVC dysfunction may cause an incoordination between neural activity and provision of oxygen and glucose. Inevitably, neural activity is reduced and thus correlates with cerebral functional impairment, manifested clinically as a cognitive decline.[47] In ESRD patients, the integrity and functional injury of cerebral vascular, endothelial dysfunction and direct neuronal toxicity,[3] resulted in changed CBF responses[16,17] and reduced neural activities,[18–23] that may eventually lead to the NVC dysfunction and cognitive impairment.

Brain regions and cognitive impairment

Based on PLSC analysis, we found that the decreased fALFF-CBF values in CG were positively correlated with lower short-term memory functional scores (SR-S) in ESRD patients, thus suggesting that the NVC dysfunction of CG may be closely related to short-term memory impairment. The NVC dysfunction of CG in ESRD patients was mainly located in the anterior cingulate cortex (ACC) and posterior cingulate cortex (PCC). As the posterior default-mode network (DMN) hub, individuals with ESRD showed decreased functional connectivity in the PCC, which were closely related to vital cognitive functions, such as memory.[22,48] In fact, posterior leukinopathy is not uncommon in ESRD patients who undergo dialysis,[49] and PCC, as the posterior DMN hub, is often involved in the complications of cerebrovascular autoregulation damage, endothelial injury, and elevated plasma concentration of natriuretic peptide.[48] Moreover, some investigators have also highlighted the importance of progressive functional connectivity density decreased of the ACC in patients with ESRD from healthy controls to minimal nephrotic encephalopathy that may be correlated to cognitive deficits.[50] Our results indicated that the mismatch between the requirement of oxygen and the blood supply (the NVC dysfunction) in the CG may be related to short-term memory impairment.

In addition, we found the brain regions of NVC dysfunction in ESRD patients were mainly located in FuG, MFG, SFG, and MTG. The FuG is a brain region involved in high-level visual processing, category identification, and object recognition of complex stimuli, such as those expressed by faces. The SFG is a key node of dorsal attention networks involved in basic cognitive selection of sensory information and response.[51] The MFG is a significant part of dorsolateral prefrontal cortex (DLPFC) that is most typically associated with executive functions including selective attention and verbal working memory.[52] More recently, Li and his colleagues[18] found that ESRD patients had reduced spontaneous neural activity in DLPFC based on the use of rs-fMRI and ALFF analysis, which was strongly associated with short-term verbal memory deficits. From our neuropsychological assessment, ESRD patients have poorer performances in global cognitive function, verbal working memory, short-term memory, long-term memory, attention, and executive function compared with HCs. Taken together, although we did not find a close relationship between the NVC dysfunction in these brain regions such as MTG, FuG, SFG and the cognitive scale, the NVC dysfunction in ESRD-vulnerable brain regions may reflect the pattern of brain functional injury to a certain extent.

Relationship among the NVC pattern's alteration, short-term memory deficit, and dialysis adequacy in ESRD patients

Understanding and exploring the mechanisms of the NVC in health and disease may help us identify potential therapies to delay or prevent the dysfunction of NVC in the treatment of vascular brain diseases, including vascular dementia and Alzheimer's disease. Applying PLSC and mediation analysis, we examined the correlation among the changed NVC biomarkers, clinical characteristics, and cognitive variables in patients with ESRD. Our results proved that the relationship between Kt/V and short-term memory deficits of ESRD patients was partially mediated by the fALFF-CBF alteration of the CG, suggesting that ESRD-related neurovascular biomarkers could be combined for monitoring dialysis efficacy and progression of cognitive impairment. A Kt/V value is used to quantify HD treatment adequacy. Patients with ESRD usually have a high level of uremic toxin (particularly urea) that is considered to be a significant risk factor for cognitive impairment.[53] The Kt/V value shows how much urea has been effectively removed according to the measurements of blood urea levels before and after treatment. Based on the results of our mediation analysis, the low level of Kt/V in ESRD patients may lead to the accumulation of uricemia toxin in the blood, thereby aggravating the NVC dysfunction in ESRD-related neurovascular brain regions thus causing more severe short-term memory damage.

Limitations

There are several issues that should be addressed. First, our study results were limited to a small sample size, which may affect the comprehensive interpretation of the NVC dysfunction in ESRD patients related to cognitive impairment. Second, we only conducted a cross-sectional study on ESRD patients. Subsequent studies should focus on the longitudinal explanation of the dynamic changes in cognitive impairment during long-term maintenance hemodialysis and the potential NVC mechanism of ESRD patients. Third, we did not exclude the influence of drugs on cognitive assessment, such as antihypertensive drugs,[54] erythropoietin,[55] and Vitamin D,[56] which may affect cognitive function. Fourth, the HCs data lacked blood analyses. Fifth, we did not assess the degree of postdialysis fatigue[57] and pain[58] in ESRD patients, so it was unclear what their effects were on cognitive function and NVC dysfunction.

Conclusion

Patients with ESRD have NVC dysfunctions in multiple brain regions that were closely related to multidimensional cognitive impairment. More importantly, the dialysis adequacy had a significant influence on regional NVC dysfunction and associated cognitive impairment evidenced in ESRD patients. This suggests that ESRD-related neurovascular biomarkers could be combined for monitoring the efficacy of dialysis and the progression of cognitive impairment. These findings may provide a novel multimodal neuroimaging evidence to improve the understanding of neurovascular mechanisms in ESRD patients and related cognitive impairment.

Funding

The author(s) disclosed receipt of the following financial support for the research, authorship, and/or publication of this article: National Natural Science Foundation of China (Grant No. 82071879, 81901821), the Science and Technology Plan of Shaanxi Province (Grant 2019SF-209), the Science and Technology Million Project of Inner Mongolia Medical University (YKD2020KJBW(LH)021), and the Fundamental Research Funds for the Central Universities (Grant Nos. JB211203, XJS201207).

Declaration of conflicting interests

The author(s) declared no potential conflicts of interest with respect to the research, authorship, and/or publication of this article.

Authors' contributions

Peng Li and Junya Mu made a substantial contribution to the concept, design, analysis and draft the article. Xueying Ma, Dun Ding, Shaohui Ma, and Huawen Zhang revised the article and interpreted the data. Jixin Liu and Ming Zhang provided intellectual content of critical importance to the work described. All authors also approved the version to be published.

Supplemental material

Supplemental material for this article is available online.

References

1. van Dijk PC, Zwinderman AH, Dekker FW, et al. Effect of general population mortality on the North-South mortality gradient in patients on replacement therapy in Europe. *Kidney Int* 2007; 71: 53–59.
2. Kurella Tamura M and Yaffe K. Dementia and cognitive impairment in ESRD: diagnostic and therapeutic strategies. *Kidney Int* 2011; 79: 14–22.
3. Bugnicourt JM, Godefroy O, Chillon JM, et al. Cognitive disorders and dementia in CKD: the neglected kidney-brain axis. *J Am Soc Nephrol* 2013; 24: 353–363.
4. Cheung KL and LaMantia MA. Cognitive impairment and mortality in patients receiving hemodialysis: implications and future research avenues. *Am J Kidney Dis* 2019; 74: 435–437.
5. Kalirao P, Pederson S, Foley RN, et al. Cognitive impairment in peritoneal dialysis patients. *Am J Kidney Dis* 2011; 57: 612–620.
6. Lu R, Kiernan MC, Murray A, et al. Kidney-brain crosstalk in the acute and chronic setting. *Nat Rev Nephrol* 2015; 11: 707–719.
7. Zhao Q, Yan T, Chopp M, et al. Brain-kidney interaction: renal dysfunction following ischemic stroke. *J Cereb Blood Flow Metab* 2020; 40: 246–262.
8. Tryc AB, Alwan G, Bokemeyer M, et al. Cerebral metabolic alterations and cognitive dysfunction in chronic kidney disease. *Nephrol Dial Transpl* 2011; 26: 2635–2641.
9. De Backer WA, Verpooten GA, Borgonjon DJ, et al. Hypoxemia during hemodialysis: effects of different membranes and dialysate compositions. *Kidney Int* 1983; 23: 738–743.
10. Phillips AA, Chan FH, Zheng MM, et al. Neurovascular coupling in humans: physiology, methodological advances and clinical implications. *J Cereb Blood Flow Metab* 2016; 36: 647–664.
11. Iadecola C. The neurovascular unit coming of age: a journey through neurovascular coupling in health and disease. *Neuron* 2017; 96: 17–42.
12. Zlokovic BV. Neurovascular pathways to neurodegeneration in Alzheimer's disease and other disorders. *Nat Rev Neurosci* 2011; 12: 723–738.
13. Najjar S, Pearlman DM, Devinsky O, et al. Neurovascular unit dysfunction with blood-brain barrier hyperpermeability contributes to major depressive disorder: a review of clinical and experimental evidence. *J Neuroinflammation* 2013; 10: 142.
14. Zhu J, Zhuo C, Xu L, et al. Altered coupling between resting-state cerebral blood flow and functional connectivity in schizophrenia. *Schizophr Bull* 2017; 43: 1363–1374.
15. Hu B, Yan LF, Sun Q, et al. Disturbed neurovascular coupling in type 2 diabetes mellitus patients: evidence from a comprehensive fMRI analysis. *Neuroimage Clin* 2019; 22: 101802.
16. Cheng BC, Chen PC, Chen PC, et al. Decreased cerebral blood flow and improved cognitive function in patients with end-stage renal disease after peritoneal dialysis: an arterial spin-labelling study. *Eur Radiol* 2019; 29: 1415–1424.
17. Jiang XL, Wen JQ, Zhang LJ, et al. Cerebral blood flow changes in hemodialysis and peritoneal dialysis patients: an arterial-spin labeling MR imaging. *Metab Brain Dis* 2016; 31: 929–936.
18. Li P, Ding D, Ma XY, et al. Altered intrinsic brain activity and memory performance improvement in patients with end-stage renal disease during a single dialysis session. *Brain Imag Behav* 2018; 12: 1640–1649.
19. Liang X, Wen J, Ni L, et al. Altered pattern of spontaneous brain activity in the patients with end-stage renal disease: a resting-state functional MRI study with regional homogeneity analysis. *PLoS One* 2013; 8: e71507.
20. Luo S, Qi RF, Wen JQ, et al. Abnormal intrinsic brain activity patterns in patients with end-stage renal disease undergoing peritoneal dialysis: a resting-state functional MR imaging study. *Radiology* 2016; 278: 181–189.
21. Mu J, Chen T, Liu Q, et al. Abnormal interaction between cognitive control network and affective network in patients with end-stage renal disease. *Brain Imag Behav* 2018; 12: 1099–1111.
22. Ni L, Wen J, Zhang LJ, et al. Aberrant default-mode functional connectivity in patients with end-stage renal disease: a resting-state functional MR imaging study. *Radiology* 2014; 271: 543–552.
23. Shi Y, Tong C, Zhang M, et al. Altered functional connectivity density in the brains of hemodialysis end-stage renal disease patients: an in vivo resting-state functional MRI study. *PLoS One* 2019; 14: e0227123.
24. Ogawa S, Lee TM, Kay AR, et al. Brain magnetic resonance imaging with contrast dependent on blood oxygenation. *Proc Natl Acad Sci USA* 1990; 87: 9868–9872.
25. Kisler K, Nelson AR, Rege SV, et al. Pericyte degeneration leads to neurovascular uncoupling and limits oxygen supply to brain. *Nat Neurosci* 2017; 20: 406–416.
26. Davis DH, Creavin ST, Yip JL, et al. Montreal cognitive assessment for the diagnosis of Alzheimer's disease and other dementias. *Cochr Datab Syst Rev* 2015; CD010775.

27. Zhao Q, Guo Q, Liang X, et al. Auditory verbal learning test is superior to Rey-Osterrieth complex figure memory for predicting mild cognitive impairment to Alzheimer's disease. *Car* 2015; 12: 520–526.
28. Bowie CR and Harvey PD. Administration and interpretation of the trail making test. *Nat Protoc* 2006; 1: 2277–2281.
29. Lovibond PF and Lovibond SH. The structure of negative emotional states: comparison of the depression anxiety stress scales (DASS) with the beck depression and anxiety inventories. *Behav Res Ther* 1995; 33: 335–343.
30. Mollayeva T, Thurairajah P, Burton K, et al. The Pittsburgh sleep quality index as a screening tool for sleep dysfunction in clinical and non-clinical samples: a systematic review and meta-analysis. *Sleep Med Rev* 2016; 25: 52–73.
31. Alsop DC, Detre JA, Golay X, et al. Recommended implementation of arterial spin-labeled perfusion MRI for clinical applications: a consensus of the ISMRM perfusion study group and the European consortium for ASL in dementia. *Magn Reson Med* 2015; 73: 102–116.
32. van Osch MJ, Teeuwisse WM, Chen Z, et al. Advances in arterial spin labelling MRI methods for measuring perfusion and collateral flow. *J Cereb Blood Flow Metab* 2018; 38: 1461–1480.
33. Chao-Gan Y and Yu-Feng Z. DPARSF: a MATLAB toolbox for "pipeline" data analysis of resting-state fMRI. *Front Syst Neurosci* 2010; 4: 13.
34. Power JD, Mitra A, Laumann TO, et al. Methods to detect, characterize, and remove motion artifact in resting state fMRI. *Neuroimage* 2014; 84: 320–341.
35. Zang Y, Jiang T, Lu Y, et al. Regional homogeneity approach to fMRI data analysis. *Neuroimage* 2004; 22: 394–400.
36. Buckner RL, Sepulcre J, Talukdar T, et al. Cortical hubs revealed by intrinsic functional connectivity: mapping, assessment of stability, and relation to Alzheimer's disease. *J Neurosci* 2009; 29: 1860–1873.
37. Zuo XN, Ehmke R, Mennes M, et al. Network centrality in the human functional connectome. *Cereb Cortex* 2012; 22: 1862–1875.
38. Fan L, Li H, Zhuo J, et al. The human brainnetome atlas: a new brain atlas based on connectional architecture. *Cereb Cortex* 2016; 26: 3508–3526.
39. Good CD, Johnsrude IS, Ashburner J, et al. A voxel-based morphometric study of ageing in 465 normal adult human brains. *Neuroimage* 2001; 14: 21–36.
40. Good CD, Johnsrude I, Ashburner J, et al. Cerebral asymmetry and the effects of sex and handedness on brain structure: a voxel-based morphometric analysis of 465 normal adult human brains. *Neuroimage* 2001; 14: 685–700.
41. Tsapanou A, Habeck C, Gazes Y, et al. Brain biomarkers and cognition across adulthood. *Hum Brain Mapp* 2019; 40: 3832–3842.
42. Zang YF, He Y, Zhu CZ, et al. Altered baseline brain activity in children with ADHD revealed by resting-state functional MRI. *Brain Dev* 2007; 29: 83–91.
43. Zou QH, Zhu CZ, Yang Y, et al. An improved approach to detection of amplitude of low-frequency fluctuation (ALFF) for resting-state fMRI: fractional ALFF. *J Neurosci Methods* 2008; 172: 137–141.
44. Liang X, Zou Q, He Y, et al. Coupling of functional connectivity and regional cerebral blood flow reveals a physiological basis for network hubs of the human brain. *Proc Natl Acad Sci USA* 2013; 110: 1929–1934.
45. Shabir O, Berwick J and Francis SE. Neurovascular dysfunction in vascular dementia, Alzheimer's and atherosclerosis. *BMC Neurosci* 2018; 19: 62.
46. Kisler K, Nelson AR, Montagne A, et al. Cerebral blood flow regulation and neurovascular dysfunction in Alzheimer disease. *Nat Rev Neurosci* 2017; 18: 419–434.
47. Tarantini S, Tran CHT, Gordon GR, et al. Impaired neurovascular coupling in aging and Alzheimer's disease: contribution of astrocyte dysfunction and endothelial impairment to cognitive decline. *Exp Gerontol* 2017; 94: 52–58.
48. Lu H, Gu Z, Xing W, et al. Alterations of default mode functional connectivity in individuals with end-stage renal disease and mild cognitive impairment. *BMC Nephrol* 2019; 20: 246.
49. Krishnan AV and Kiernan MC. Neurological complications of chronic kidney disease. *Nat Rev Neurol* 2009; 5: 542–551.
50. Zhang XD, Wen JQ, Xu Q, et al. Altered long- and short-range functional connectivity in the patients with end-stage renal disease: a resting-state functional MRI study. *Metab Brain Dis* 2015; 30: 1175–1186.
51. Corbetta M and Shulman GL. Control of goal-directed and stimulus-driven attention in the brain. *Nat Rev Neurosci* 2002; 3: 201–215.
52. Curtis CE and D'Esposito M. Persistent activity in the prefrontal cortex during working memory. *Trends Cogn Sci* 2003; 7: 415–423.
53. Watanabe K, Watanabe T and Nakayama M. Cerebrorenal interactions: impact of uremic toxins on cognitive function. *Neurotoxicology* 2014; 44: 184–193.
54. Birkenhager WH and Staessen JA. Antihypertensives for prevention of Alzheimer's disease. *Lancet Neurol* 2006; 5: 466–468.
55. Lee ST, Chu K, Park JE, et al. Erythropoietin improves memory function with reducing endothelial dysfunction and amyloid-beta burden in Alzheimer's disease models. *J Neurochem* 2012; 120: 115–124.
56. Latimer CS, Brewer LD, Searcy JL, et al. Vitamin D prevents cognitive decline and enhances hippocampal synaptic function in aging rats. *Proc Natl Acad Sci USA* 2014; 111: E4359–E4366.
57. Bossola M and Tazza L. Postdialysis fatigue: a frequent and debilitating symptom. *Semin Dial* 2016; 29: 222–227.
58. Brkovic T, Burilovic E and Puljak L. Risk factors associated with pain on chronic intermittent hemodialysis: a systematic review. *Pain Pract* 2018; 18: 247–268.